



# A NOVEL AND ROBUST APPROACH FOR DENOISING OF COMPUTED TOMOGRAPHY IMAGES USING DUAL TREE COMPLEX WAVELET PACKETS AND EMPIRICAL MODE DECOMPOSITION TOWARDS OPTIMIZATION

<sup>1</sup>A.VELAYUDHAM, <sup>2</sup>R.KANTHAHEL

<sup>1</sup>Assistant Professor (SG), Department of IT, Cape Institute of Technology, Levengipuram-627114, India

<sup>2</sup>Professor and Head, Department of ECE, Velammal Engineering College, Chennai-66, India

E-mail: <sup>1</sup>[a.velayudham@gmail.com](mailto:a.velayudham@gmail.com), <sup>2</sup>[r\\_kanthavel@yahoo.com](mailto:r_kanthavel@yahoo.com)

## ABSTRACT

Computed tomography (CT) images are usually corrupted by several noises from the measurement process complicating the automatic feature extraction and analysis of clinical data. To attain the best possible diagnosis it is very vital that medical images be clear, sharp, and free of noise and artifacts. While the techniques for obtaining digital medical images continue to improve, ensuing in images of higher and higher resolution and quality, noise remains an issue for many medical images. Removing noise in these medical images remains as one of the key challenges in the study of medical imaging. A range of literatures have been developed towards solving the hitch of medical images denoising which is a significant stage in an automatic diagnosis system. In this research paper, we propose a new image denoising technique using Dual Tree Complex Wavelet Packets, Empirical Mode Decomposition and Sobel operator. Here, histon process is used in order to surmount the smoothing filter type and it will not affect the lower dimensions. We have taken into consideration two noises, Gaussian and salt & pepper for proposed technique. The performance of the proposed image denoising technique is assessed on the five CT images for the parameters, PSNR and SDME. For performance assessment studies & comparison, our proposed denoising technique is compared with the existing work in assorted noise levels. From the obtained outcomes, we can conclude that the proposed denoising technique have shown better values for the SDME of 67.8798 and PSNR of 24.841 for salt & pepper noise which is very superior compared to existing methods.

**Keywords:** CT, EMD, Dual Tree Complex Wavelet Packet (DTCWP), PSNR, SDME

## 1. INTRODUCTION

A traditional crisis in image processing is Noise reduction. Digital image reconstruction is a robust means by which the underlying images masked in blurry and noisy data can be exposed. The major confront in input data is the sensitiveness to noise measurement, which can be magnified firmly, resulting in huge artifacts in the reconstructed image. By reconstructing the permitted images, this intricacy can be defeated. Since they can analyze with less corruption, transmission of video images requires less significance of noise removal comparing with the voice data. However, if we lose a particular area in case of medical images, then it will result in immense disaster similar to death. Therefore, denoising of medical images is further essential which leads physician for precise analysis

of diseases. Medical images like X-RAY, CT (Computed Tomography), MRI (Magnetic Resonance Imaging), PET (Positron Emission Tomography) and SPECT (Single Photon Emission Computed Tomography) encompass diminutive information about heart, brain, nerves and more. For determining the internal structure of an object, X-ray Computed Tomography (CT) is a powerful method [18]. As such it determines application, e.g. in the non-destructive testing of a variety of materials. From a huge number of systematic observations at diverse viewing angles, the CT image is derived, and with the support of a computer (Radon transform) the final CT image is then reconstructed.

It is unfeasible to rescue a human being from harmful effects, when these medical images are corrupted by noise. In both Image Processing and

Biomedical Engineering, CT image Denoising is a significant research theme. In the case of CT, numerous mathematical and medical applications [11]-[14] [23] can be applied to conclude whether the normal tissue has been infected by the mutations of the cancer cell. The disease diagnosis procedure has been made more efficient by denoising the CT images where the noise is removed. The denoised images encompass a prominent level of elevation in its PSNR values, ensuring a smoother image for diagnosis function. For developing the quality of the CT images, a variety of methods have been established. By using filters and wavelet denoising methods, Denoising has been achieved. Since they are accomplished of suppressing noise, recent wavelet thresholding based denoising methods have proved capable, during the conservation of the high frequency signal details [2]. However, by standard wavelet thresholding methods, the local space-scale information of the image is not adaptively considered. The threshold at certain scale is a constant for all wavelet coefficients in standard wavelet thresholding based noise reduction methods [20]. In a few applications, wavelet based denoising has been showed efficient. Fundamentally, the noisy image is transformed into the wavelet domain, then the wavelet coefficients are shifted to soft or hard thresholding, and the result has been inverse-transformed in the final step [16-17] [24].

In this work, we proposed an efficient denoising technique using DTCWP and EMD for denoising of an image. Here, histon process is used in order to overcome the smoothing filter type and it will not affect the lower dimensions. Then DTCWP and EMD are used for the image denoising and image enhancement phase. Finally, PSNR and SDME are used for the evaluation matrices. The rest of the paper is organized as follows: a brief review of some of the literature works in denoising technique is presented in Section 2. Contribution is discussed in section 3. The proposed CT image denoising technique is detailed in Section 4. The experimental results and performance evaluation discussion is provided in Section 5. Finally, the conclusions are summed up in Section 6.

## 2. EXISTING APPROACHES

A lot of researches have been developed for the denoising in various images. A few of the modern related works concerning the denoising papers are reviewed in this section.

In recent years, medical image denoising plays a significant role in modern applications and especially, denoising of CT-scan images have been

received a great deal of attention among the researches due to its wide applicability and abundant growth of medical image-based system. In general, most of the researchers have used the wavelet-based de-noising technique in order to remove the noisy pixels from the CT-scan images. Here, the denoisy strategy is applied on the wavelet domain so as to better estimate the original image rather than applying the spatial domain. Most of the techniques presented in the literature for the last decades have been used wavelet- thresholding method to compute the noisy free image because well suitability of wavelets in de-noising. According to this, Tischenko et al. [1] proposed a structure-saving noise minimizing technique using the correlations between two images for calculation of threshold in the wavelet domain. The fact that unlike actual signal, noise is more or less uncorrelated over time has motivated their approach. Assuming the patient remains still, two projection radiography images taken in quick succession has been considered to have the same information but with uncorrelated noise between the images. A wavelet transformation has been used to partition both images and correlation measurement has been performed using the cosine of the angle between the approximated gradient vectors of the two images. Without modifying the coefficients with high correlation they have weighted down the coefficients that have low correlation. The noise suppressed image obtained as the output of the inverse wavelet transformation still included all correlated structures.

In addition, Anja Borsdorf et al. [2] by discovering a method to obtain spatially identical input images in case of CT have reduced the problems that occur in this technique. Direct acquisition of the two images by independent reconstructions from the projections measured at the two detectors has been a possibility with the modern generation dual-source CT-scanners (DSCT). Also, they have proposed a correlation based similarity measurement coefficient. The basis for their local similarity measurement has been built by the pixel areas from the approximation images of the preceding decomposition level, which by means of the calculation of the wavelet transformation directly alters the value of a corresponding detail coefficient. Furthermore, use of diverse wavelet transformations with diverse properties for two input images based noise reduction has been analyzed. They have utilized the averaged and weighted wavelet coefficients of the input images for reconstructing the final noise-suppressed image. These two techniques motivated to continue my

research on the CT-scan image denoising with the aid of wavelets that is a well-known technique for de-noising for the recent years.

G.Y. Chen and B.Kegl [4] have presented an image denoising method by incorporating the dual-tree complex wavelets into the ordinary ridgelet transform. The approximate shift invariant property of the dual-tree complex wavelet and the high directional sensitivity of the ridgelet transform made the method a very good choice for image denoising. They applied the digital complex ridgelet transform to denoise some standard images corrupted with additive white noise. Experimental results showed that the method outperformed VisuShrink, the ordinary ridgelet image denoising, and wiener2 filter both in terms of peak signal-to-noise ratio and in visual quality. In particular, their method was persevered sharp edges better while removing white noise.

João M. Sanches et al. [5] have presented a Bayesian denoising algorithm which copes with additive white Gaussian and multiplicative noise described by Poisson and Rayleigh distributions. The algorithm was based on the maximum a posteriori (MAP) criterion, and edge preserving priors who avoid the distortion of relevant anatomical details. The main contribution of that paper was the unification of a set of Bayesian denoising algorithms for additive and multiplicative noise using a well-known mathematical framework, the Sylvester-Lyapunov equation, developed in the context of Control theory. Faten Ben Arfia et al. [6] have developed a method for image denoising in the filter domain based on the characteristics of the Empirical Mode Decomposition (EMD) and the wavelet technique. The proposed method used the EMD to the decomposition and double density wavelet to filter components. Their experimental results showed that those image denoising methods are more efficient than the wavelet denoising method. Finally, the PSNR (peak signal noise ratio) and the visualization of the denoising image were used as performance comparison indexes.

Guangming Zhang et al. [7] have developed a model for CT medical image de-noising, which was using independent component analysis and curvelet transform. Firstly, a random matrix was produce to separate the CT image into a separated image for estimate. Then curvelet transform was applied to optimize the coefficients. At last, the inverse of the curvelet transform was applied for image reconstruction. The de-noising image had a higher value of SNR and a lower value of MSE. Syed

Amjad Ali et al. [8] have presented an efficient noise reduction technique for CT images using window-based Multi-wavelet transformation and thresholding. The technique removed Additive white Gaussian noise from the CT images as well as it enhanced the quality of the images. The proposed technique consisted of three different stages of processing, namely, window-based multi-wavelet transformation and thresholding, reconstruction and quality enhancement. In the first two processes, the AWGN was effectively removed from CT images and the images were reconstructed. In the third process, the quality of the images was enhanced by means of filtering techniques. Hence, denoised and quality enhanced CT images were obtained using the presented multi-wavelet based denoising technique.

G. Landi and E.Loli Piccolomini [9] have modeled a denoising problem in a Bayesian statistical setting by a non-negatively constrained minimization problem, where the objective function was constituted by a data fitting term, the Kullback-Leibler divergence, plus a regularization term, the Total Variation function, weighted by a regularization parameter. Aim of the paper was to develop an efficient numerical method for the solution of the constrained problem. The method was a Newton projection method, where the inner system was solved by the Conjugate Gradient method, preconditioned and implemented in an efficient way for this specific application. The numerical results on simulated and real medical images proved the effectiveness of the method, both for the accuracy and the computational cost.

### 3. PROPOSED METHOD

The main contribution of the proposed denoising technique is Dual tree complex wavelet packet decomposition (DTCWPD) and Empirical mode decomposition (EMD) are used for the denoising technique. The hybrid techniques are chosen because of the ill-suitability of dual tree complex wavelet to represent long oscillatory patterns in images with abundant textures and directly eliminate the noisy pixels based on the threshold. Also, the DTCWPD is a flexible method for image denoising that utilize the combined advantages of wavelet packet and dual tree complex wavelet. Additionally, Empirical mode decomposition (EMD) is a technique, to overcome the main drawback of complex wavelet and Fourier transform approaches.

Commonly, noise reduction is an important part of image processing domain. An image is always

affected by noise in its capture, acquisition and processing. This denoising is employed to improve the quality of an image corrupted by a lot of noise due to the undesired conditions for image acquisition. A variety of literatures have been presented in recent times. In this paper, we have designed an efficient denoising technique using Dual tree complex wavelet packet decomposition (DTCWPD) and Empirical mode decomposition (EMD). The overall diagram of proposed denoising technique is given in Figure 1.

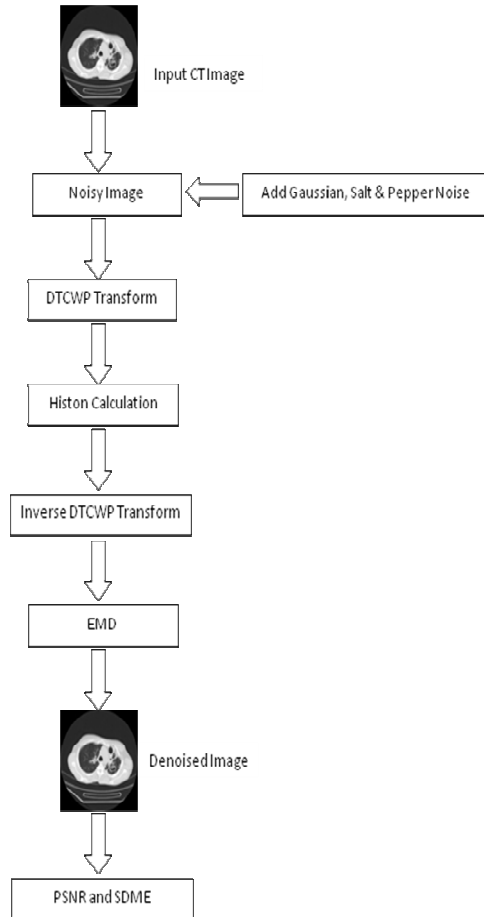


Figure 1: Proposed Denoising Method

The overall proposed denoising process is composed into two phases:

- ❖ Noise area identification phase
- ❖ Denoising image phase

### 3.1 Noise Area Identification Phase

Let  $I(p, q)$  be an original CT image of size  $M \times N$ . Here, the noises (Gaussian and salt & pepper) are applied for the input original CT image, we obtain  $N[I(p, q)]$ . Where,  $N[I(p, q)]$  is the noised image. In Gaussian noise, each pixel in the

image is changed from its original value by a (usually) small amount. In salt and pepper noise (sparse light and dark disturbances), pixels in the image are very different in color or intensity from their surrounding pixels; the defining characteristic is that the value of a noisy pixel bears no relation to the color of surrounding pixels. Generally this type of noise will only affect a small number of image pixels. When viewed, the image contains dark and white dots, hence the term salt and pepper noise. The denoising steps are given by:

#### 3.1.1 Applying DTCWP

Firstly, DTCWP is applied on the noised image  $N[I(p, q)]$ . Decompose the noise image  $N[I(p, q)]$  into four sub-bands, such as HH, LL, HL and LH with the aid of the Dual tree complex wavelet packet transform and we obtain  $FW[I(p, q)]$ . Where,  $FW[I(p, q)]$  is forward Dual tree complex wavelet packet transform output. In this stage, DTCWP is used to overcome the limitations of the classical DWT, such as shift-sensitivity and directional selectivity problems. Here, *shift-sensitivity* is small shifts in the input image can cause main variations in the distribution of energy between DWT coefficients at different scales. *Directional selectivity* means the wavelet filters are separable and real. DTCWP has solved the above two disadvantages in this step. There are two process involved in the DTCWP transform, such as, forward Dual tree complex wavelet packet and inverse Dual tree complex wavelet packet. In this step, we have applied forward Dual tree complex wavelet packet. The forward Dual tree complex wavelet packet requires three Perfect Reconstruction filters (PR) in this stage. The tree structure of the DTCWP is given in Figure 2.

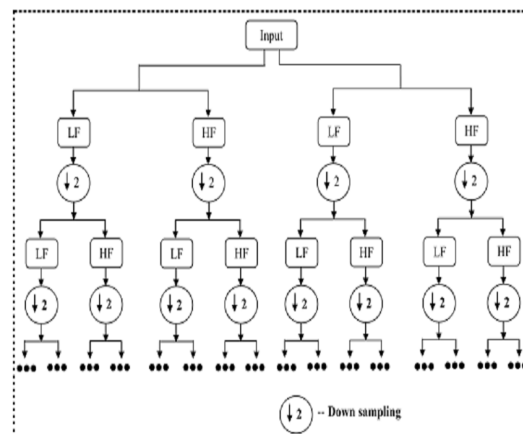


Figure 2: DTCWP transform tree model

### 3.1.2 Applying Histon Calculation

After applying forward Dual tree complex wavelet packet, the histon calculation is performed. This process is used in order to smoothing filter type and it will not affect the lower dimensions. Initially, in resultant image  $FW[I(p, q)]$  finding the difference between the neighbors and updating the values of neighbors by keeping threshold values. By changing the pixel values and finding the difference between the nearest neighbors is the process behind the noise removal process. Thus the process continues till our eligibility criteria occur. The important steps of histon process are given by:

- ❖ Using the difference between the nearest neighbors, calculate the pixel value.
- ❖ we utilize the formula to find the difference between the nearest neighbors for all the pixels values as follows

$$\text{Difference of a particular pixel} = \text{Nearest neighbor 1} - \text{Nearest neighbor 2} \quad (1)$$

- ❖ After finding the pixels values update the pixels values by setting a threshold. Here we used the threshold value as greater than 1 or less than 1.
- ❖ Then to find the intensity values of a pixel, we find the difference between the nearest neighbors for the particular pixel values. Using the same formula (1) we find the intensity values of a pixel.
- ❖ After finding the intensity values of a pixel, we have to update the values in the image by setting the threshold. The threshold value is greater than or less than 0.5.
- ❖ Update the count values in the particular intensity value of a pixel and we check one by one via histogram and plot the values.
- ❖ Here, with the difference between the neighbors the intensity values of a pixel is calculated. By keeping threshold, the intensity value of a pixel is calculated. (i.e.) if the calculated difference between the neighbors is greater than one means replace the pixel value with 2 and if the calculated difference between the neighbors is less than one means replace the pixel value with 0.
- ❖ The above process repeats until the eligibility criterion occurs. In our process it takes 200 iterations to complete the process. After completing every iteration the image  $FW[I(p, q)]$  is represented as  $FW[I(p, q)]'$ ,  $FW[I(p, q)]''$ ,  $FW[I(p, q)]'''$ , ... and so on.

By using the above process, we compute and rearrange the pixel values to find the noisy areas without affecting the lower dimensional areas. If the count value is greater than the neighbors then we instruct to update the pixel intensity value. Thus after completing the rearranging process and having applied inverse DTCWP, we obtain some intensity values of a noisy image  $IW[I(p, q)]$ . i.e., an inverse DTCWP is then applied to the rest of coefficients to reconstruct the data. Then, the noisy image is given to the empirical mode decomposition process for image enhancement purpose.

### 3.2 Denoising Phase

#### 3.2.1 Applying EMD

After inverse process, the EMD is applied on the  $IW[I(p, q)]$  image. Empirical mode decomposition [3] is an efficient filtering technique to reduce the noise and image smoothing. Firstly, the  $IW[I(p, q)]$  image is vectorized and given into EMD. Then, in our experimentation, EMD was performed on each channel vector separately and the facet of decomposing a signal into Intrinsic Mode Function (IMF) is utilized in the denoising purpose. The EMD process is to perform sift operations on the original data series until the final series are stationary. The EMD process is shown in Figure 3. The sifting process begins from the image  $IW(p, q)$  and the initial input to the EMD to the process is followed by

$$\text{input}_{mn}(p, q) = IW(p, q) \quad (2)$$

Where  $m$  is used as index to show the  $m^{\text{th}}$  IMF, and  $m$  represents iteration number of the current step while  $(p, q)$  denotes the spatial image location.

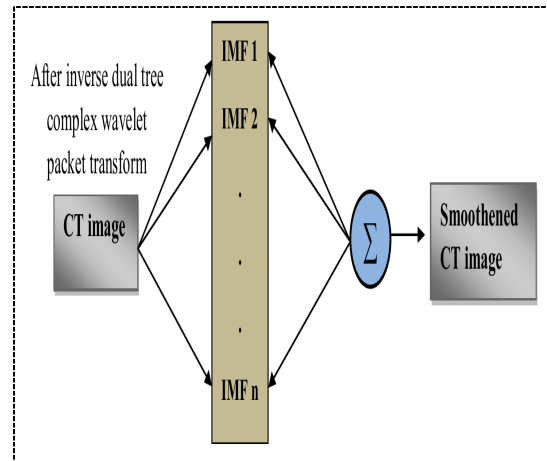


Figure 3: EMD Process



The decomposition process of EMD is as follows:

- Calculate all points of local maxima and all points of the local minima of  $input_{mn}(p, q) = IW(p, q)$  for every position.
- Interpolate the local maxima to form an upper envelope ( $e_{\max}(p, q)$ ).
- Interpolate the local minima to form a lower envelope ( $e_{\min}(p, q)$ ).
- Calculate the mean of upper and lower envelope for each position

$$(e\_Mean_{mn}(p, q)) = \frac{e_{\max}(p, q) + e_{\min}(p, q)}{2} \quad (3)$$

- From the input signal (vector), subtract the mean envelope

$$h_{mn}(p, q) = input_{lk}(p, q) - (e\_mean_{mn}(p, q)) \quad (4)$$

This is a one iteration of the sifting process. The next step is to check if the signal (vector)  $h_{mn}(p, q)$  from step (e) is an IMF or not.

- Calculate the stopping criterion

$$eps = \frac{\sum_{p=1}^H \sum_{q=1}^W |(e\_mean_{mn}(p, q))|}{H \times W} \quad (5)$$

Where,  $W$  and  $H$  denotes dimensional of the image and  $eps$  denotes stopping criterion. Check if envelope mean satisfies the iteration stop criterion for the current IMF. If the stop criterion for the current IMF falls below a small threshold such that  $eps < \kappa$ , here  $\kappa$  is the small threshold the sifting process is stopped for the current IMF is obtained as  $IMF_m(p, q) = h_{mn}(p, q)$ . If the stop criterion is not met, the next iteration is started with  $input_{m(n+1)}(p, q) = h_{mn}(p, q)$  and this process is repeated from step 1 to find the current IMF.

- If the current IMF acquired correctly, the residue signal  $R_m(p, q)$  is calculated as  $R_m(p, q) = input_{l1}(p, q) - IMF_m(p, q)$ . If the residue does not contain any more extreme points the EMD decomposition process is terminated. Otherwise the next IMF is computed from step (a) using the residue as input, i.e.  $input_{(m+1),1}(p, q) = R_m(p, q)$ .

The EMD process decomposes the noised image into several IMFs, and final residue  $R_m$ . The resultant image is actually sum of these components.

$$IW_{EMD}(p, q) = R_m(p, q) + \sum_{m=1}^M IMF_m(p, q) \quad (6)$$

From the equation (6), the image,  $IW_{EMD}(p, q)$  is obtained. But,  $IW_{EMD}(p, q)$  contains white pixels. For this purpose, we are going to use edge detection technique. Edges are usually local changes of intensity in an image. Here, Sobel edge detector is used and the specialty of Sobel edge operator is that it detects thicker edges.

### 3.2.2 Applying Sobel Operator

The Sobel detector is incredibly sensitive to noise in pictures, it effectively highlights them as edges. In the Sobel edge detection, the operator consists of a pair 8\*8 blocks, one estimating the gradient in the x-direction (columns) and the other estimating the gradient in the y-direction (rows). Convolution mask is usually much smaller than the actual image. As a result, the mask is slid over the image, manipulating a square of pixels at a time. The edge detected image can be obtained from the Sobel gradient by using a threshold value. If the Sobel gradient values are lesser than the threshold value then replaces it with the threshold value,

$$\text{If } f < \text{threshold value then, } f = \text{threshold value} \quad (7)$$

In Sobel edge detector, the region based edge detection process consists of threshold with values less than 5 and hence the values less than or equal to five are removed and then the image splits into two blocks as  $G_P$ ,  $G_Q$ .

Here the main process is by using a count values, we will rearrange the data. If the count value is same means we will take the average of all other data and change the particular pixel value. If the count value in the block is not same means we will find the difference between the nearest neighbors and update the particular value. Thus the process continues till the eligibility criterion occurs.

After splitting the blocks into 8\*8, the edge detection process takes place. The magnitude of the gradient is calculated using the formula as follows,

$$|G| = \sqrt{G_P^2 + G_Q^2} \quad (8)$$

The direction of the gradient is calculated using the formula

$$\theta = \tan^{-1} \left( \frac{G_Q}{G_P} \right) \quad (9)$$

Where,  $G$  is the gradient magnitude

$\theta$  is the gradient direction.

$G_P$  And  $G_Q$  are the blocks which we split and then the Sobel edge detector process takes

place. After finding the magnitude and direction of the gradient in Sobel edge detector the intensity values of a pixel is updated.

In above process repeat the steps until the results are obtained. This process is done until it reaches the threshold. If it is reached, then PSNR and SDME value is to be found out. To find the PSNR and SDME values of an image we have to calculate the mean square error value. Thus the PSNR and SDME values for different iterations are shown in the table below. The peak signal to noise ratio is the ratio of maximum possible pixel in the image to the ratio of mean square value. Although PSNR can measure the intensity difference between two images, it is well-known that it may fail to describe the visual perception quality of the image. Here in our proposed technique we find the PSNR and SDME values by calculating the difference between the pixels in the image.

#### 4. IMPLEMENTATION METHODOLOGY

This section presents the results obtained from the experimentation and its detailed discussion about the results. The proposed approach of image denoising is experimented with the CT medical images and the result is evaluated with the PSNR and SDME.

##### 4.1 Simulation Environment

The proposed method is implemented in a Windows machine having a configuration of Intel (R) core I5 processor, 3.20 Ghz, 4 GB RAM and the operation system platform Is Microsoft Windows7 Professional. We have used Matlab latest version (7.12) for this proposed technique.

**Dataset description:** For our proposed denoising technique, we have taken five different CT images and these images are publicly available. The five CT images are given in Figure 4.

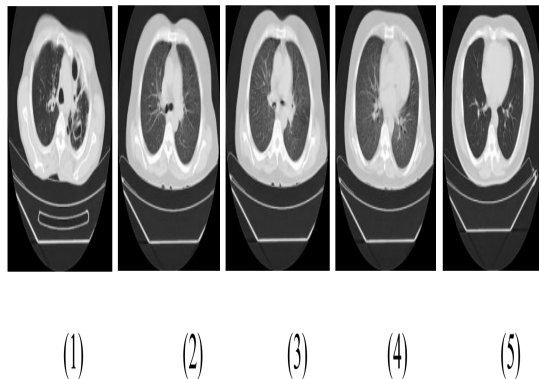


Figure 4: CT Images for our proposed method

##### 4.2 Evaluation Metrics

The formulae used to compute the evaluation metrics PSNR and SDME values are given as follows,

##### 4.2.1 Peak Signal to Noise Ratio (PSNR)

The formula for PSNR value computation is,

$$PSNR = 10 \log_{10} \frac{E_{\max}^2 \times I_w \times I_h}{\sum (I_{xy} - I_{xy}^*)^2}$$

Where,  $I_w$  and  $I_h \rightarrow$  Width and height of the denoised image

$I_{xy} \rightarrow$  Original image pixel value at coordinate  $(x, y)$

$I_{xy}^* \rightarrow$  Denoised image pixel value at coordinate  $(x, y)$

$E_{\max}^2 \rightarrow$  Largest energy of the image pixels

##### 4.2.2 Second Derivative Measure of Enhancement (SDME)

The formula for SDME value computation [22] is,

$$SDME = -\frac{1}{k_1 k_2} 20 \ln \left| \frac{I_{\max;k,l} - 2I_{center;k,l} + I_{\min;k,l}}{I_{\max;k,l} + 2I_{center;k,l} + I_{\min;k,l}} \right|$$

Where the denoised image is divided into  $(k_1 \times k_2)$  blocks with odd size,  $I_{\max;k,l}$  and  $I_{\min;k,l}$  correspond to the maximum and minimum values of pixels in each block whereas  $I_{center;k,l}$  is the value of the intensity of the pixel in the center of each block.

##### 4.2.3 Experimental Results

In this section, we have five CT images and two noises (Gaussian and salt & pepper) are taken for proposed denoising technique. Here, we show three different CT images and the corresponding noise image and noise variance levels, noised images and denoised images. Hence these images were given as input for denoising and the step by step process of our proposed technique is shown in the Fig below. Table 1 to 3 shows the (i) input image (ii) Noise image (iii) shows the noise variance level (iv) Noised image of the CT lungs image and (iv) denoised images.

TABLE 1: RESULTS OF PROPOSED DENOISING TECHNIQUE FOR CT IMAGE 1

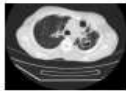

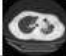

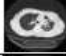
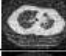



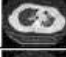



Input	Noise	Noise variance level	Noised Image	Denoised Image
	Gaussian	0.02		
		0.04		
		0.06		
	Salt & papper	0.02		
		0.04		
		0.06		

TABLE 2: RESULTS OF PROPOSED DENOISING TECHNIQUE FOR CT IMAGE 2










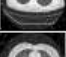





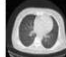

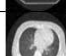
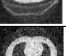
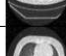



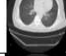

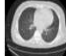
Input	Noise	Noise Variance level	Noised Image	Denoised Image
	Gaussian	0.02		
		0.04		
		0.06		
	Salt & papper	0.02		
		0.04		
		0.06		

TABLE 3: RESULTS OF PROPOSED DENOISING TECHNIQUE FOR CT IMAGE 3

Input	Noise	Noise variance level	Noised Image	Denoised Image
	Gaussian	0.02		
		0.04		
		0.06		
	Salt & papper	0.02		
		0.04		
		0.06		

## 5. IMPLEMENTATION RESULTS

In this paper, we have compared our proposed denoising technique against existing technique (Sachin D *et al.* [10]) with five CT images. The performance analysis has been made by plotting the graphs of evaluation metrics such as PSNR and SDME as shown in Figures 5 to 24. By analyzing the plotted graph, the performance of the proposed technique has significantly improved the PSNR and SDME compared with existing technique [10].

In 1<sup>st</sup> image, the performance graphs are plotted and they are given in Fig 5 to 8. In PSNR graph, the proposed denoising technique achieved the PSNR value of 21.1287 which is high compared with the PSNR value of existing technique (16.718) for Gaussian noise. In SDME graph, proposed denoising technique achieved the SDME value of 46.73, which is high compared with the SDME value of existing technique (43.736) for Gaussian noise. The proposed denoising technique achieved the PSNR value of 21.9445 which is high compared with the PSNR value of existing technique (21.63) for salt & pepper noise. In SDME graph, proposed denoising technique achieved the SDME value of 43.10, which is high compared with the SDME value of existing technique (38.09) for salt & pepper noise.

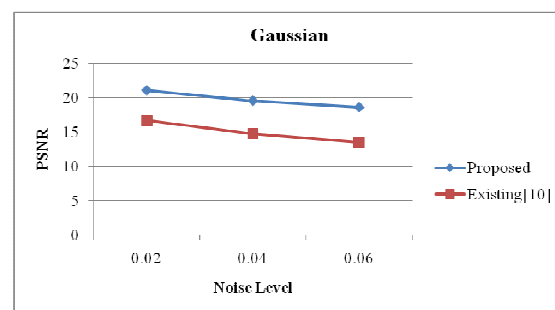


Figure 5: PSNR graph of Gaussian noise for CT image 1

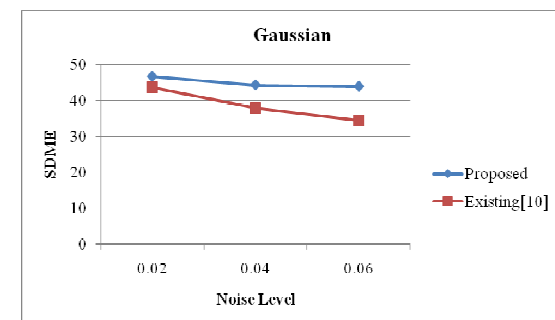


Figure 6: SDME graph of Gaussian noise for CT image 1



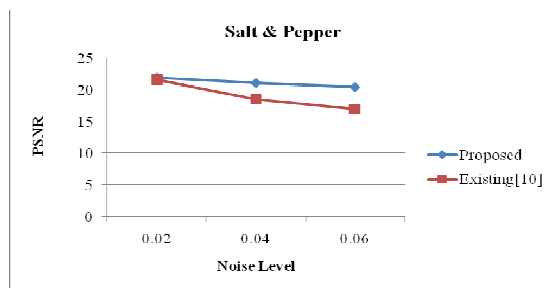


Figure 7: PSNR graph of salt & pepper noise for CT image 1

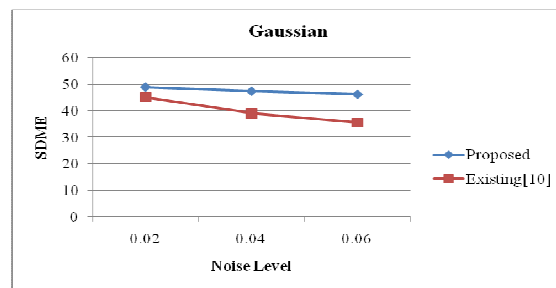


Figure 10: SDME graph of Gaussian noise for CT image 2

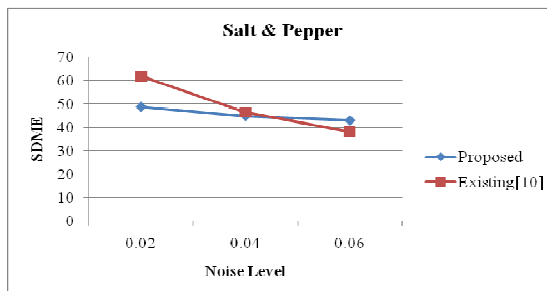


Figure 8: SDME graph of salt & pepper noise for CT image 1

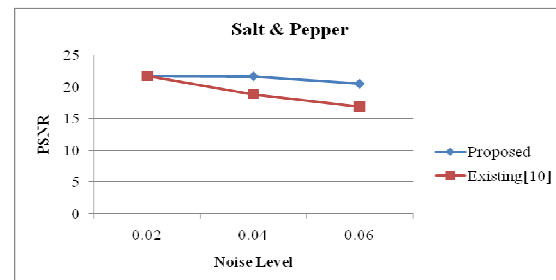


Figure 11: PSNR graph of salt & pepper noise for CT image 2

In 2<sup>nd</sup> image, the performance graphs are plotted and they are given in Fig 9 to 12. The proposed denoising technique achieved the PSNR value of 21.318 which is high compared with the PSNR value of existing technique (16.80) for Gaussian noise. In SDME graph, proposed denoising technique achieved the SDME value of 48.97, which is high compared with the SDME value of existing technique (45.13) for Gaussian noise. The proposed denoising technique achieved the PSNR value of 21.75 which is high compared with the PSNR value of existing technique (18.911) for salt & pepper noise. In SDME graph, proposed denoising technique achieved the SDME value of 44.012, which is high compared with the SDME value of existing technique (38.214) for salt & pepper noise.

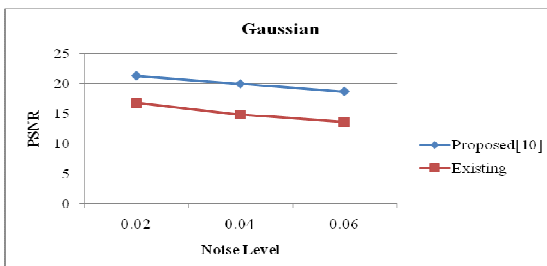


Figure 9: PSNR graph of Gaussian noise for CT image 2

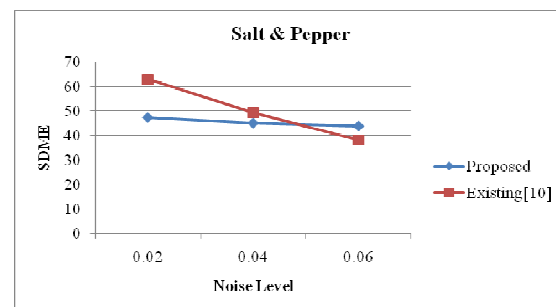


Figure 12: SDME graph of salt & pepper noise for CT image 2

In 3<sup>rd</sup> image, the performance graphs are plotted and they are given in Fig 13 to 16. In PSNR graph, the proposed denoising technique achieved the PSNR value of 21.206 which is high compared with the PSNR value of existing technique (16.756) for Gaussian noise. In SDME graph, proposed denoising technique achieved the SDME value of 48.32, which is high compared with the SDME value of existing technique (39.84) for Gaussian noise. The proposed denoising technique achieved the PSNR value of 22.5698 which is high compared with the PSNR value of existing technique (21.736) for salt & pepper noise. In SDME graph, proposed denoising technique achieved the SDME value of 43.7783, which is high compared with the SDME

value of existing technique (39.7519) for salt & pepper noise.

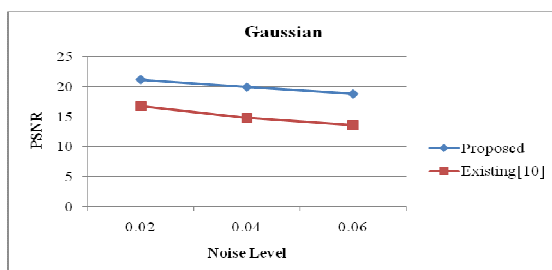


Figure 13: PSNR graph of Gaussian noise for CT image 3

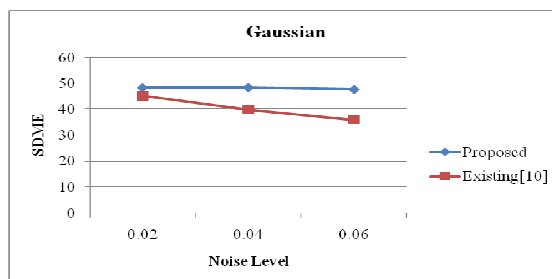


Figure 14: SDME graph of Gaussian noise for CT image 3

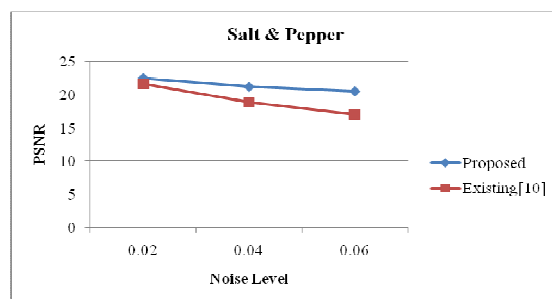


Figure 15: PSNR graph of salt & pepper noise for CT image 3

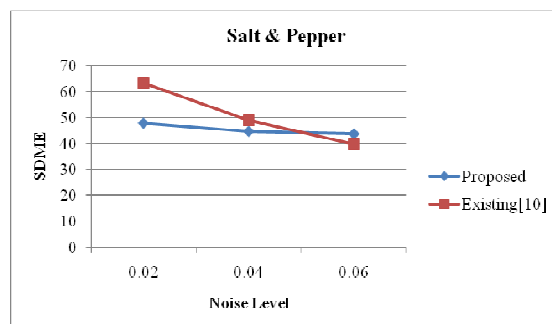


Figure 16: SDME graph of salt & pepper noise for CT image 3

In 4<sup>th</sup> image, the performance graphs are plotted and they are given in Fig 17 to 20. The proposed denoising technique achieved the PSNR value of 21.3496 which is high compared with the PSNR value of existing technique (16.7834) for Gaussian noise. In SDME graph, proposed denoising technique achieved the SDME value of 49.7599, which is high compared with the SDME value of existing technique (45.405) for Gaussian noise. The proposed denoising technique achieved the PSNR value of 22.1813 which is high compared with the PSNR value of existing technique (21.8897) for salt & pepper noise. In SDME graph, proposed denoising technique achieved the SDME value of 43.8492, which is high compared with the SDME value of existing technique (38.2939) for salt & pepper noise.

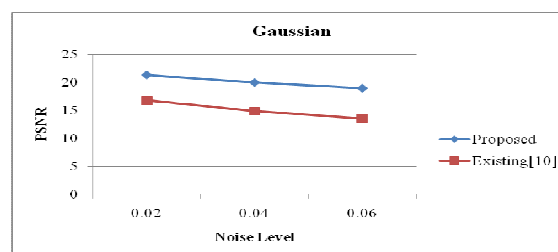


Figure 17: PSNR graph of Gaussian noise for CT image 4

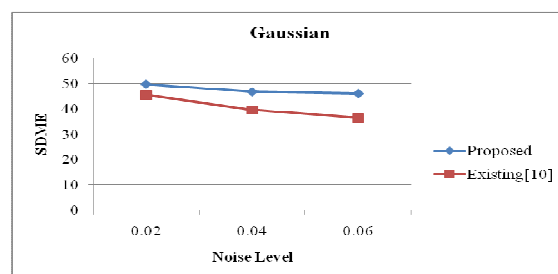


Figure 18: SDME graph of Gaussian noise for CT image 4

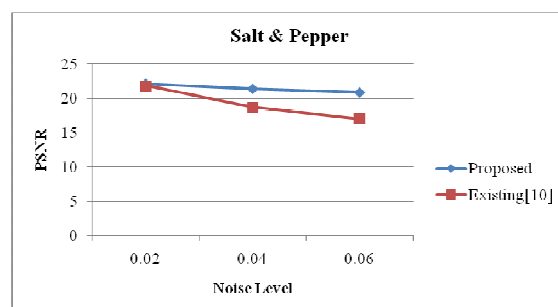


Figure 19: PSNR graph of salt & pepper noise for CT image 4

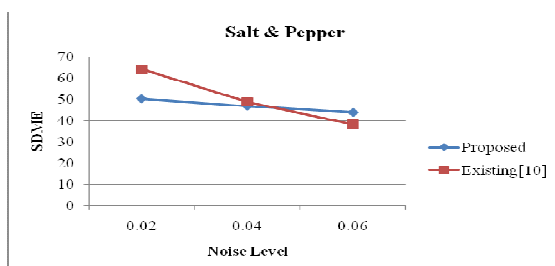


Figure 20: SDME graph of salt & pepper noise for CT image 4

In 5<sup>th</sup> image, the performance graphs are plotted and they are given in Fig 21 to 24. In PSNR graph, the proposed denoising technique achieved the PSNR value of 21.1233 which is high compared with the PSNR value of existing technique (16.7386) for Gaussian noise. In SDME graph, proposed denoising technique achieved the SDME value of 47.992, which is high compared with the SDME value of existing technique (43.3181) for Gaussian noise. The proposed denoising technique achieved the PSNR value of 21.7314 which is high compared with the PSNR value of existing technique (21.4638) for salt & pepper noise. In SDME graph, proposed denoising technique achieved the SDME value of 42.0401, which is high compared with the SDME value of existing technique (38.366) for salt & pepper noise. Totally, from the Table 4, the proposed denoising technique is achieved better results when compared existing technique [10].

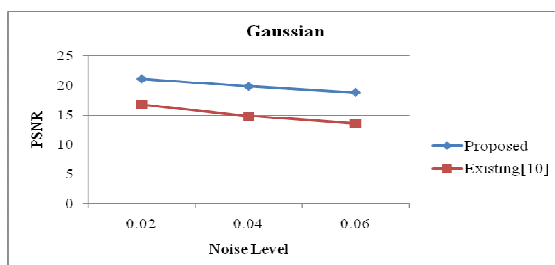


Figure 21: PSNR graph of Gaussian noise for CT image 5

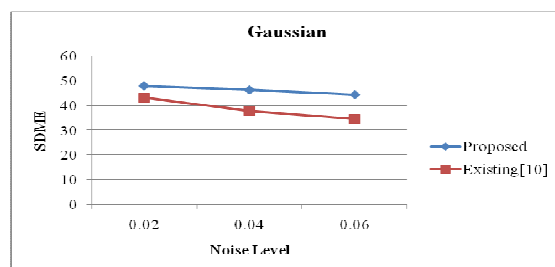


Figure 22: SDME graph of Gaussian noise for CT image 5

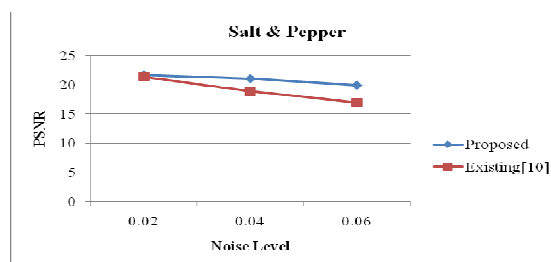


Figure 23: PSNR graph of salt & pepper noise for CT image 5

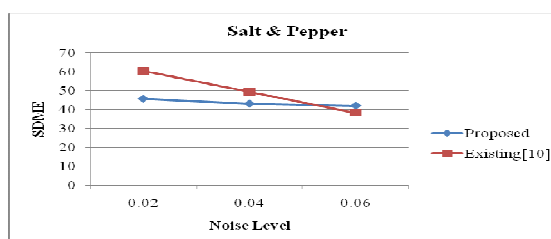


Figure 24: SDME graph of salt & pepper noise for CT image 5

Table 4: Comparison Of Psnr Values Of Proposed Method With Existing Method For Gaussian Noise






Input CT Image	Noise level	Proposed	Existing [10]
	0.02	21.1287	16.7166
	0.04	19.6213	14.7828
	0.06	18.646	13.5612
	0.02	21.3186	16.8026
	0.04	19.9728	14.8172
	0.06	18.6979	13.6043
	0.02	21.206	16.7567
	0.04	19.9561	14.8153
	0.06	18.828	13.5965
	0.02	21.3496	16.7834
	0.04	19.9989	14.856
	0.06	18.9786	13.5704
	0.02	21.1233	16.7386
	0.04	19.8723	14.8244
	0.06	18.8407	13.5808

Table 4 shows the comparison values of Peak Signal to Noise Ratio (PSNR) for different noise variance levels for gaussian noise between the proposed method and the existing method. Table 5 shows the comparison values of Second Derivative Measure of Enhancement (SDME) for different noise variance levels for gaussian noise between the proposed method and the existing method.

Table 5: Comparison Of Sdme Values Of Proposed Method With Existing Method For Gaussian Noise

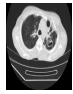




Input CT Image	Noise level	Proposed	Existing [10]
	0.02	46.7269	43.7036
	0.04	44.338	37.9114
	0.06	43.9474	34.4204
	0.02	48.9719	45.1277
	0.04	47.3975	38.9988
	0.06	46.162	35.6109
	0.02	48.2659	45.1306
	0.04	48.3279	39.8488
	0.06	47.5855	35.9237
	0.02	49.7599	45.4059
	0.04	46.7261	39.5777
	0.06	46.0037	36.3572
	0.02	47.992	43.3181
	0.04	46.4375	37.8772
	0.06	44.4947	34.7142

Table 6: Comparison Of Psnr Values Of Proposed Method With Existing Method For Salt And Pepper Noise

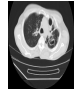




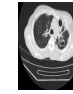




Input CT Image	Noise level	Proposed	Existing [10]
	0.02	21.9445	21.634
	0.04	21.0776	18.567
	0.06	20.4357	17.0057
	0.02	24.841	21.8661
	0.04	21.7599	18.918
	0.06	20.5562	16.9189
	0.02	22.5698	21.7306
	0.04	21.2678	18.8978
	0.06	20.5852	17.0635
	0.02	22.1813	21.8897
	0.04	21.4148	18.7489
	0.06	20.8899	17.0178
	0.02	21.7314	21.4638
	0.04	21.1082	18.9884
	0.06	19.9906	16.9854

Table 6 shows the comparison values of Peak Signal to Noise Ratio (PSNR) for different noise variance levels for salt and pepper noise between the proposed method and the existing method.

Table 7 shows the comparison values of Second Derivative Measure of Enhancement (SDME) for different noise variance levels for salt and pepper noise between the proposed method and the existing method.

Table 7: Comparison Of Sdme Values Of Proposed Method With Existing Method For Salt And Pepper Noise

Input CT Image	Noise level	Proposed	Existing [10]
	0.02	67.8798	52.0768
	0.04	64.9669	46.527
	0.06	43.101	38.0931
	0.02	67.5065	52.9996
	0.04	65.2206	49.4154
	0.06	44.0129	38.2141
	0.02	67.9266	63.3859
	0.04	64.7767	59.0446
	0.06	43.7783	39.7519
	0.02	64.3396	54.1842
	0.04	68.8235	48.8421
	0.06	43.8492	38.2939
	0.02	65.8095	50.4402
	0.04	63.1082	49.5018
	0.06	42.0401	38.365

## 6. CONCLUSION

Image denoising is a familiar preprocessing step in many CT image processing and analysis tasks, such as segmentation, registration or parametric image synthesis. In recent years, various image denoising techniques are developed. In this paper, we propose a new image denoising technique using EMD and Dual Tree Complex Wavelet Packets. Here, histon process is used in order to overcome the smoothing filter type and it will not affect the lower dimensions. We have used two noises, like as Gaussian and salt & pepper for proposed technique. The performance of the proposed image denoising technique is evaluated on the five CT images using the PSNR and SDME. For comparison analysis, our proposed denoising technique is compared with the existing work in various noise levels. The above calculations are being performed on an image of resolution 512×512 and work is being done to remove Gaussian and salt & pepper noise of the images and future plan is to make it valuable for



different resolution and for different size of images.

## REFERENCES:

- [1] O. Tischenko, C. Hoeschen, and E. Buhr, "An artifact-free structure saving noise reduction using the correlation between two images for threshold determination in the wavelet domain," in *Medical Imaging 2005: Image Processing. Proceedings of the SPIE.*, J. M. Fitzpatrick and J. M. Reinhardt, Eds., vol. 5747, pp. 1066-1075, April 2005.
- [2] Anja Borsdorf, Rainer Raupach, Thomas Flohr and Joachim Hornegger, "Wavelet based Noise Reduction in CT-Images using Correlation Analysis", *IEEE transactions on medical imaging*, Vol. 27, No.12, 2008.
- [3] N. Huang, Z. Shen, S. Long, M. Wu, H. Shih, Q. Zheng, N. Yen, C. Tung, H. Liu, The empirical mode decomposition and Hilbert spectrum for nonlinear and non-stationary time series analysis, *Proceedings of the Royal Society of London*, Vol: 454, pp: 903-995, 1998.
- [4] G.Y. Chen, B.Kégl, "Image denoising with complex ridgelets," *Pattern Recognition*, Vol. 40, pp.578-585, 2007.
- [5] João M. Sanches, Jacinto C. Nascimento, and Jorge S. Marques "Medical Image Noise Reduction Using the Sylvester-Lyapunov Equation," *IEEE Transactions On Image Processing*, Vol. 17, No. 9, September 2008.
- [6] Faten Ben Arfia, Mohamed Ben Messaoud, Mohamed Abid, "A New Image denoising Technique Combining the Empirical Mode Decomposition with a Wavelet Transform Technique," *17th International Conference on Systems, Signals and Image Processing*, 2010.
- [7] Guangming Zhang, Zhiming Cui, Jianming Chen and Jian Wu, "CT Image De-noising Model Based on Independent Component Analysis and Curvelet Transform," *Journal Of Software*, Vol. 5, No. 9, September 2010.
- [8] Syed Amjad Ali, Srinivasan Vathsal, K. Lal kishore, "An Efficient Denoising Technique for CT Images using Window-based Multi-Wavelet Transformation and Thresholding," *European Journal of Scientific Research*, Vol.48, No.2, pp.315-325, 2010.
- [9] G. Landi, E.Loli Piccolomini, "An efficient method for nonnegatively constrained Total Variation-based denoising of medical images corrupted by Poisson noise," *Computerized Medical Imaging and Graphics*, Vol.36, pp. 38- 46, 2012.
- [10] Sachin D, Ruikar and Dharmpal D Doye, "Wavelet Based Image Denoising Technique", *International Journal of Advanced Computer Science and Applications*, Vol. 2, No. 3, pp. 49-53, 2011.
- [11] Shanshan Wang, Yong Xia, Qiegen Liu, Jianhua Luo, Yuemin Zhu, David Dagan Feng, "Gabor feature based nonlocal means filter for textured image denoising," *J. Vis. Commun. Image R.*, Vol.23, pp.1008-1018, 2012.
- [12] Ehsan Nadernejad, Mohsen Nikpour, "Image denoising using new pixon representation based on fuzzy filtering and partial differential equations," *Digital Signal Processing*, Vol.22, pp.913-922, 2012.
- [13] V Naga Prudhvi Raj, Dr T Venkateswarlu, "Denoising of medical images using dual tree complex wavelet transform," *Procedia Technology*, Vol.4, pp.238-244, 2012.
- [14] Jianhua Luo, Yuemin Zhu, "Denoising of medical images using a reconstruction-average mechanism," *Digital Signal Processing*, Vol.22, pp.337-347, 2012.
- [15] R. Sivakumar, "Denoising of computer tomography images using curvelet transform", *ARNP-JEAS*, Vol.2, No.1, pp. 21 - 26, February 2007.
- [16] Sudipta Roy, Nidul Sinha, Asoke K. Sen, "A New Hybrid Image Denoising Method", *International Journal of Information Technology and Knowledge Management*, Vol. 2, No. 2, pp. 491 - 497, December 2010.
- [17] Shutao Li, Leyuan Fang and Haitao Yin, "An Efficient Dictionary Learning Algorithm and Its Application to 3-D Medical Image Denoising", *IEEE Transactions On Biomedical Engineering*, Vol. 59, No. 2, February 2012.
- [18] V N Prudhvi Raj and Dr. T Venkateswarlu, "Denoising Of Medical Images Using Image Fusion Techniques", *Signal & Image Processing: An International Journal*, Vol. 3, No. 4, August 2012.
- [19] Syed Amjad Ali, Srinivasan Vathsal, Lal Kishore, "CT Image denoising technique using GA aided window-based multiwavelet transformation & thresholding with the incorporation of an effective quality enhancement method", *International Journal of Digital Content Technology and its Applications (IJDCTA)*, Vol.4, No.4, pp. 75 - 87, July 2010.



- [20] Abdolhossein Fathi and Ahmad Reza Naghsh-Nilchi, "Efficient Image Denoising Method Based on a New Adaptive Wavelet Packet Thresholding Function", *IEEE Transactions On Image Processing*, Vol. 21, No. 9, September 2012.
- [21] Sudipta Roy, Nidul Sinha, Asoke K Sen, "An Efficient Denoising Model based on Wavelet and Bilateral Filters", *International Journal of Computer Applications*, Vol. 53, No. 10, pp. 28-35, September 2012.
- [22] Karen Panetta, Yicong Zhou, Sos Agaian, and Hongwei Jia, "Nonlinear Unsharp Masking for Mammogram Enhancement, " *IEEE Transactions On Information Technology In Biomedicine*, Vol. 15, No. 6, November 2011.
- [23] Zhao Juanjuan, Yang Jianfeng, Qiang Yan, Wang Quan, "Lung CT Image Segmentation Based on Combined Multi-Scales Watershed Method and Region Growing Method," *Image Segmentation, Lung Segmentation, Multi Scales, Region Growing, Watershed*, Vol 8 N. 2 (Part B), pp.587-592, February 2013.
- [24] K. Selva Bhuvaneswari, P. Geetha, "Tumor, Edema and Atrophy Segmentation of Brain MRI with Wavelet Transform and Semantic Features, " *Segmentation, Pathological tissues, Artificial Neural Network*, White Matter, Gray Matter, Cerebrospinal Fluid, Tumor, Edema, Atrophy, Vol.8 No.6, pp. 1243-1254, June 2013.